Monitoring TriAcylGlycerols Accumulation by Atomic Force Microscopy Based Infrared Spectroscopy in Streptomyces Species for Biodiesel Applications

ARTICLE *in* JOURNAL OF PHYSICAL CHEMISTRY LETTERS · JANUARY 2014

Impact Factor: 7.46 · DOI: 10.1021/jz402393a

4 AUTHORS:

Ariane Deniset
Université Paris-Sud 11
35 PUBLICATIONS **264** CITATIONS
SEE PROFILE

Craig Prater
Anasys Instruments
64 PUBLICATIONS **3,396** CITATIONS
SEE PROFILE

Marie-Joelle Virolle
Université Paris-Sud 11
37 PUBLICATIONS **670** CITATIONS
SEE PROFILE

Alexandre Dazzi
Université Paris-Sud 11
56 PUBLICATIONS **696** CITATIONS
SEE PROFILE

THE JOURNAL OF PHYSICAL CHEMISTRY Letters

Letter

pubs.acs.org/JPCL

Monitoring TriAcylGlycerols Accumulation by Atomic Force Microscopy Based Infrared Spectroscopy in *Streptomyces* Species for Biodiesel Applications

Ariane Deniset-Besseau,*[,†] Craig B. Prater,[‡] Marie-Joëlle Virolle,[§] and Alexandre Dazzi[†]

[†]Laboratoire de Chimie-Physique, Université Paris-Sud-CNRS UMR 8000, Orsay, France

[‡]Anasys Instruments, 325 Chapel Street, Suite 100, Santa Barbara, California 93101, United States

[§]Institut de Génétique et Microbiologie, Groupe "Métabolisme Energétique des *Streptomyces*", Université Paris-Sud-CNRS UMR 8621, Orsay, France

ABSTRACT: An atomic force microscope coupled with a tunable infrared laser source (AFM-IR) was used to measure the size and map the distribution of oil inclusions inside of microorganism without staining or other special sample preparation. The microorganism under study is *Streptomyces*, a soil bacterium that possesses the capability, under some specific nutritional conditions, to store its carbon source into TriAcylGlycerols, a potential direct source of biodiesel.

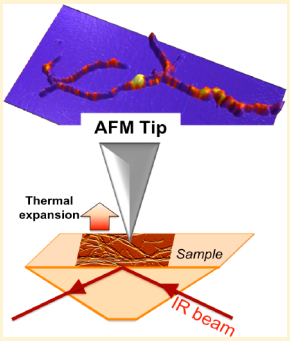

SECTION: Biophysical Chemistry and Biomolecules

Biodiesel is an old fuel. Indeed, between 1893 and 1897, Rudolf Diesel fueled his prototype engine with peanut oil. However, because at this time petroleum deposits were huge and kept petrodiesel cheap for decades, biofuels were largely forgotten. With the recent increase of oil prices, along with growing concern about global warming, biofuels and among them bio-oils regained popularity. Unlike underground oil reserves, biofuels are a renewable resource, and their carbon balance is favorable. Combustion is more complete than that in petrodiesel with fewer particles, and emissions are less toxic.[1]

First-generation bio-oils are being produced from seeds of oleaginous plants (rapeseed, soybean, sunflower, etc.). This highly integrated agroindustrial sector yields useful oils for alimentation, biodiesel, cosmetics, painting, lubricants for high precision mechanics, and so forth. However, the mobilization of agricultural fields for biodiesel production, in a context of a growing world population to feed, has been the subject of controversial debates. As a consequence, producing bio-oils by fermentation of oleaginous microorganisms constitutes an interesting alternative to the mobilization of agricultural lands for biofuel production.

A recently identified candidate to generate bio-oils is the bacterium *Streptomyces*,[2] a soil organism that can store an excess of carbon in TriAcylGlycerols (TAGs),[3] a ready-to-use source for biodiesel production.[4,5]

Those bacteria present numerous advantages for the development of a new industrial sector dedicated to the production of bio-oils. Indeed, their conditions of fermentation at an industrial scale have been mastered for decades by the pharmaceutical industry because they are the main producers of antibiotics.[6] In some specific nutritional conditions, some natural strains are able to accumulate up to 50% of their dry weight as TAG. Interestingly, recent research has demonstrated a tight link between storage lipids' metabolism and antibiotic production in those bacteria.[7] Furthermore, those filamentous bacteria possess all of the enzymatic systems to degrade organic waste (lignocellulose, pulp, etc.) and therefore are able to use the leftovers from agriculture and the food industry for their growth and TAG accumulation. The genome of many species (over 25) has been sequenced, and all of the genetic tools are available to implement requested genetic engineering strategies in those bacteria.

In this study, our goal was to evaluate, at the subcellular scale, the size/shape and localization of storage lipid inclusions in two *Streptomyces* strains, *Streptomyces lividans* and *Streptomyces coelicolor*.[8] *S. lividans* and *S. coelicolor* both have the genetic capability to produce three well-known antibiotics; *S. coelicolor* produces them abundantly and *S. lividans* quite weakly.

In a previous study, the global TAG content of those strains was easily and precisely quantified using FTIR measurements and thin layer chromatography,[7] revealing that *S. coelicolor* has a very low TAG content whereas *S. lividans* has an high TAG

Received: November 6, 2013
Accepted: January 27, 2014
Published: January 27, 2014

content, demonstrating a reverse correlation between the TAG content and antibiotic production.

This was possible because TAG molecules show a specific response in the mid-infrared (IR) region (see Figure 1), quite distinct from that of the other cellular constituants.

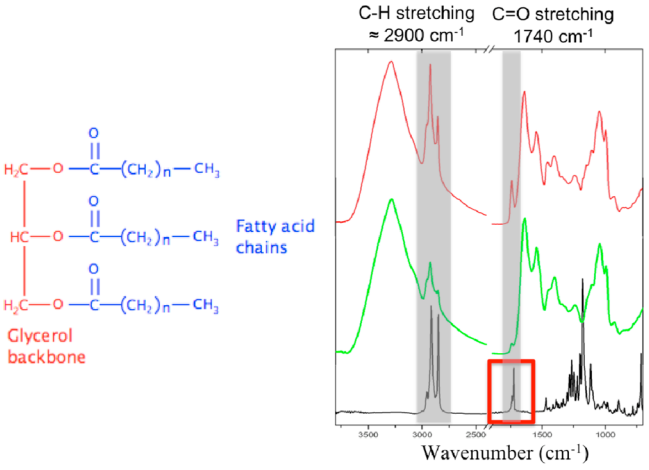

Figure 1. The general chemical formula of TAG and a typical FTIR spectrum of commercial TAG powder (black line) compared with the FTIR spectrum of the two strains *S. lividans* (red line) and *S. coelicolor* (green line).

As can be seen on the TAG IR spectrum, two spectral ranges are relevant to assess the TAG content within the cell's culture, the stretching bands of CH characteristic of fatty acid chains, more particularly 2921 cm^{-1} CH_2 antisymmetric stretching and 2852 cm^{-1} CH_2 symmetric stretching, as well as the band at 1741 cm^{-1} representing the >C═O ester stretching band of the compound. Furthermore, because the proteic content of the biomass can be directly characterized by the amplitude of the amide I absorption band (1641 cm^{-1}), all FTIR spectra were normalized to this band, allowing the comparison of the TAG content of mycelial lawns of the different *Streptomyces* strains. The difference between the two strains, in the FTIR spectra of the Figure 1, in terms of TAG content is clear and highly reproducible (the spectra were measured on three different cultures in triplicate). The C═O band intensity is higher in the strain of *S. lividans* than that in *S. coelicolor*. The behavior of the C−H band corroborates this result and confirms the high TAG content of *S. lividans*.

For the study of the local repartition of TAG inside of the cells, a combination of atomic force microscopy (AFM) and IR spectroscopy was employed in order to create subcellular chemical maps that allow label-free identification of TAG inclusions in *S. lividans* and *S. coelicolor* cytoplasm using their specific absorption properties at 1741 cm^{-1}. Protein content can be estimated at 1641 cm^{-1}.[9]

AFM-IR is a user-friendly benchtop technique that enables IR spectroscopy with a spatial resolution well below conventional optical diffraction limits. It acquires IR absorption imaging with lateral resolution down to 100 nm.[10−15] It consists of a near-field technique based on photothermal expansion of a sample due to the absorption of IR radiation.[16] Briefly, the sample is placed on an IR-transparent prism and irradiated with an IR nanosecond pulsed laser tuned to a wavelength corresponding to an absorption band of the sample. The absorbed light induced a temperature increase and consequently a rapid thermal expansion of the absorbing material. This local deformation (or expansion) was thus detected with the AFM tip in contact with the sample. This expansion is very fast. As a consequence, the cantilever undergoes a pulse and oscillates on its eigenmodes.[16,17] Mapping this oscillation amplitude versus position creates a spatially resolved map of IR absorption that can be used to localize specific chemical species with sub-100 nm lateral

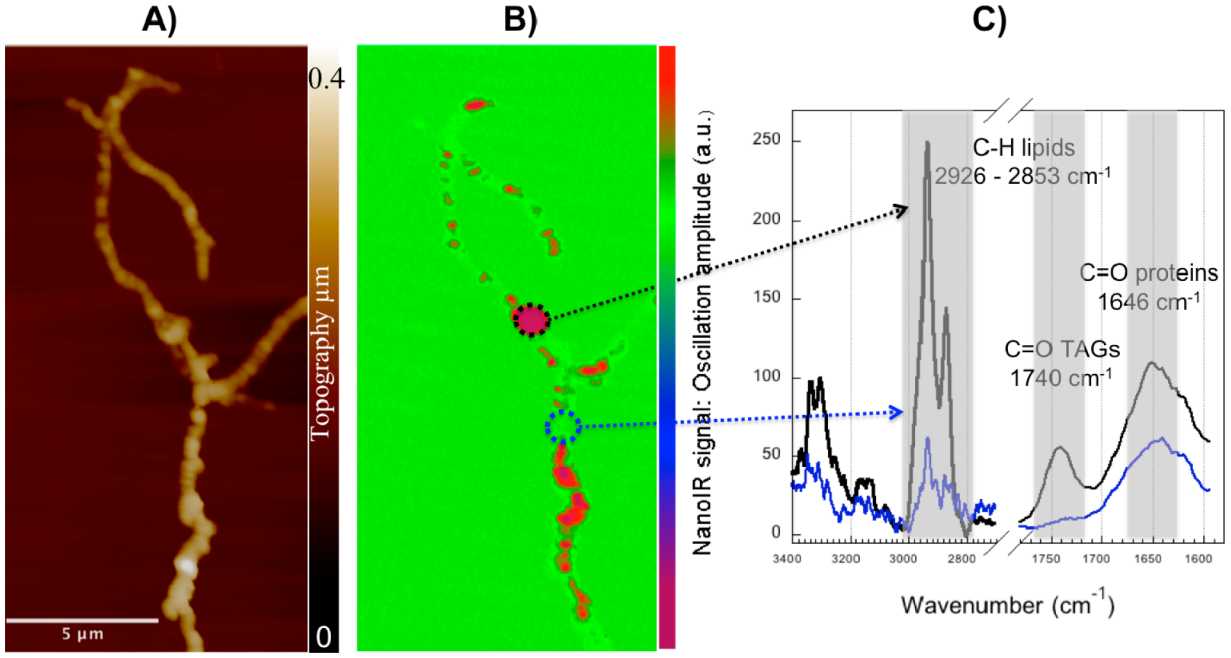

Figure 2. Results obtained with the AFM-IR system on *S. lividans*: (A) AFM topography, (B) chemical mapping at 1740 cm^{-1}, and (C) local IR spectra acquired inside of (black line) and outside of a TAG inclusion (blue line). The spectral data were all normalized to the incident power of the laser. An averaging of three spectra was done, and a five-point smoothing routine was applied.

dx.doi.org/10.1021/jz402393a | J. Phys. Chem. Lett. 2014, 5, 654−658

resolution[18] (chemical mapping at a specific wavenumber; Figure 2B). Furthermore, by measuring the amplitude of this oscillation (directly proportional to the IR absorbance[19]) as a function of laser wavelength, local chemical identification of other biological materials is possible. Hence, we obtain a complete local IR spectrum (Figure 2C).

To study the two strains of *Streptomyces*, a simple, noninvasive sample preparation technique without staining was employed (see the Experimental Methods section). Heterogeneities in size and density of TAG inclusions were noted (see Figure 3), and the chemical mappings show clear differences in TAG accumulation efficiency between the two strains.

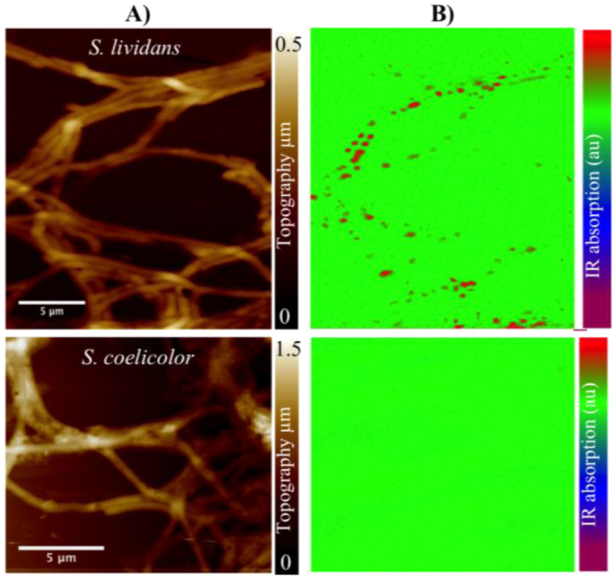

Figure 3. (A) AFM topography and (B) chemical mapping at 1740 cm^{-1} for the two strains.

It is possible to quantify the area fraction and size distribution of the TAG granules for the wild-type *S. lividans* on a typical IR imaging (Figures 2 and 3). The size of the *S. lividans* inclusions varies from 0.2 to 2 μm, whereas hardly any inclusions could be seen in *S. coelicolor* cytoplasm, or they were too small to be detected (less than 100 nm).

A first statistical study of those inclusions with MountainMaps (Digital surf) was performed in order to evaluate their repartition inside of the mycelium of *S. lividans*. The results of this statistical study are represented in Figure 4; the number of inclusions (per unit volume of mycelium analyzed) is drawn as a function of inclusions size. The majority of the inclusions (70%) shows a size between 0.2 and 0.8 μm, and 30% are between 1 and 2 μm, which is not a negligeable part of the fatty material. In Figures 2 and 3 *S. lividans* shows typical huge fatty inclusions, and if we compare the size of the granules with that of dried mycelial fragments, 40% of them are much larger than the mycelium itself (the mean size of dried mycelium of *S. coelicolor* is around 530 ± 90 nm). This fact is of most importance because the swelling might make the cell walls fragile, making the industrial extraction process easier.

The mycelium analysis was not possible with *S. coelicolor* due to the low number of fatty inclusions. In this species, this lack of inclusions is still informative and somehow confirms results obtained with classical FTIR measurements (see Figure 1). On

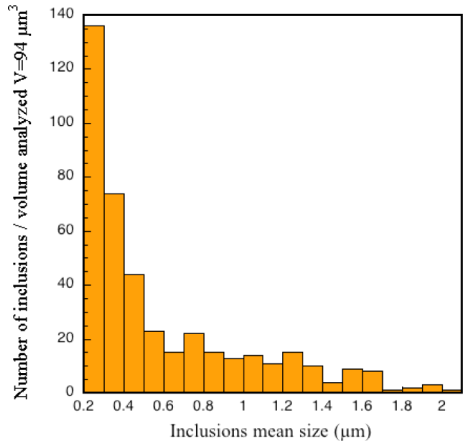

Figure 4. Size of the inclusions in *S. lividans*..

the FTIR spectra of *S. lividans*, the intensity of the ester group −1741 cm^{-1} band is clearly 3.5 times higher than that of *S. coelicolor*. More acquisitions are necessary to determine wether *S. coelicolor* contains granules of smaller size or if they are simply a rare event.

The chemical composition of the inclusions can be assessed thanks to the local spectra acquisitions (Figure 2C). Those spectra are in complete accordance with what is expected for lipid bodies;[20,21] as shown in Figure 2C, we observe locally two absorption bands (at 1740 and 1646 cm^{-1} with a resolution of 8 cm^{-1}) characteristic of TAGs and protein. Furthermore, we can assume that proteins are at the periphery and stabilize the structure of the TAG granules. The presence of TAG is also confirmed by the huge C−H bands at 2926 and 2853 cm^{-1} (instead of 2921 and 2852 cm^{-1} with FTIR), which are characteristic of the stretching of the CH_2 group in long aliphatic chains.

The AFM-IR measurements provide a free labeling means to assess the TAG content in a biological sample very quickly at a lateral spatial resolution that is commensurate with the scale of individual bacteria and lipid inclusions. It allows one to monitor the constitution of storage lipid inclusions during growth as well as in a specific part of the *Streptomyces* colonies (basal mycelium/aerial mycelium/spores).

Nevertheless, this study is at an early stage; therefore, the conclusions need to be moderate. Indeed, if small inclusions (less than 300 nm) are embedded in the mycelium, their global expansion due to the IR absorption will be modified.[14,18] This modification corresponds to an increase of the apparent diameter. The major risk is an overestimation of the size of small vesicles (100 at 300 nm) while missing the smaller ones. To reduce the effect of this overestimation, only inclusions with a minimum size of 200 nm are included in the statistical study. Thanks to the data processing, it might be possible to locate the embedded vesicles and compensate for the apparent increase of the diameter. It will be one of the next steps to refine the data processing.

This technique coupled with classical FTIR measurements constitutes a powerful tool to study TAG metabolism in *Streptomyces* and can be easily used to control the rate of lipid accumulation during the fermentation process. The development of new efficient strains in terms of lipid storage involves the construction, analysis, and validation of numerous mutants and is very time consuming. Therefore, the use of fast

dx.doi.org/10.1021/jz402393a | *J. Phys. Chem. Lett.* 2014, 5, 654−658

techniques to evaluate the lipid content in these new strains could drastically speed up the general process.

Hence, the AFM-IR technique is likely to provide new insights into the constitution of the fatty inclusions and the role of TAGs in the morphological and metabolic differentiation processes that characterize the *Streptomyces* developmental cell cycle.

Furthermore, the statistical analysis of the AFM-IR images could be of great interest. This analysis reveals the mean size of the inclusions and their repartition. In a lipid extraction process in *Streptomyces*, this information might be useful because the smaller the inclusions, even though there are many, the more difficult that it might be for their extraction to proceed. Finally, it could be a great tool to identify other organisms for biodiesel applications.

EXPERIMENTAL METHODS

Bacterial Strains and Growth Conditions. The *Streptomyces* strains were *S. lividans* and *S. coelicolor*; 10^6 spores were spread on cellophane disks laid down on the top of agar plates. The solid medium was R2YE with no addition of phosphate salts. The plates were incubated at 30 °C for 96 h.

Attenuated Total Reflectance Fourier-Transform Infrared (ATR FTIR) Measurements. Lyophilized mycelial samples of the two *Streptomyces* strains were subjected to FTIR spectroscopy using a Bruker Vertex 70 FTIR spectrometer with a diamond ATR attachment (PIKE MIRacle crystal plate diamond/ZnSe) and MCT detector with a liquid nitrogen cooling system. Scanning was conducted from 4000 to 400 cm^{-1} with a 4 cm^{-1} spectral resolution and with 100 scans averaged for each spectrum.

Sample Preparation for AFM-IR Measurements. The cell suspension of each culture was spun down by centrifugation at 5000g for 2 min, the supernatant was removed, and the cell pellet was diluted in distilled water. To obtain a cleaned preparation, this operation has been done three time to wash the bacteria correctly. Finally, a drop was deposited on ZnSe (transparent in the mid-IR) prisms for AFM-IR experiments and dried at room temperature.

To obtain our first statistical set, we performred an experiment on three different cultures. Around 20 regions of interest were probed, and for each of them, we acquired the IR mapping at 1740 cm^{-1}.

AFM-IR Technique. The first experimental setup was developed at the Centre Laser Infrarouge d'Orsay (CLIO) in the Laboratoire de Chimie Physique by using a free-electron laser as the tunable IR source. In 2010, the American company Anasys Instruments, Inc., commercialized a version of AFM-IR by using an optical parametric oscillator (OPO) as a benchtop tunable IR laser. This commercial version of the system was used for this work. Technical characteristics of the system are as follow: The OPO produced 10 ns pulses tunable between 3600 and 1000 cm^{-1} with a repetition rate of 1kHz. The power was set at 0.2 μJ per pulse for the acquisitions between 3600 and 2700 cm^{-1}. For this range, the focused laser spot diameter was around 15 μm. Between 1800 and 1500 cm^{-1}, the laser spot was around 50 μm, and the power was fixed at 3 μJ per pulse. Each IR mapping and spectrum was normalized to the incident laser power. Local spectra were collected using a 2 cm^{-1} step scan, and an average of 256 pulses was done for each data point. The spectral resolution was estimated at 8 cm^{-1} (laser pulse width). Topographic images were acquired in contact mode with cantilevers of 0.03 N/m (μmasch HQ:CSC/AIBS).

Data Processing. The AFM-IR imaging analysis was performed with MountainMaps (Digital surf). By using a threshold filter, the signal coming from the inclusions larger than 100 nm was isolated in each chemical mapping at 1740 cm^{-1}. A shape analysis algorithm was then applied. The average size of the inclusions was obtained. Thanks to the topography, the total volume of mycelium analyzed was evaluated.

AUTHOR INFORMATION

Corresponding Author

*E-mail: ariane.deniset@u-psud.fr.

Notes

The authors declare the following competing financial interest(s): The authors Ariane Deniset-Besseau and Marie-Joëlle Virolle state no conflict of interest. However, we wish to point out that Alexandre Dazzi has patented the instrument AFM-IR in 2007 (U.S. Patent 11/803421), and Craig Prater is the chief technology officer of Anasys Instrument the company that sells the commercial version of the AFM-IR.

ACKNOWLEDGMENTS

We gradefully thank Cécile Martel for the bacterial culture.

REFERENCES

(1) Hill, J.; Nelson, E.; Tilman, D.; Polasky, S.; Tiffany, D. Environmental, Economic, and Energetic Costs and Benefits of Biodiesel and Ethanol Biofuels. *Proc. Natl. Acad. Sci. U.S.A.* **2006**, *103*, 11206−11210.

(2) Holmbäck, M.; Lehestö, M.; Koskinen, P.; Selin, J. Process and Microorganisms for Production of Lipids. WO Patent WO2011/148056A1, 2011.

(3) Packter, N. M.; Olukoshi, E. R.; Tag, A. Ultrastructural Studies of Neutral Lipid Localisation in Streptomyces. *Arch. Microbiol.* **1995**, *164*, 420−427.

(4) Subramaniam, R.; Dufreche, S.; Zappi, M.; Bajpai, R. Microbial Lipids from Renewable Resources: Production and Characterization. *J. Ind. Microbiol. Biotechnol.* **2010**, *37*, 1271−1287.

(5) Shi, S.; Valle-Rodríguez, J.; Siewers, V.; Nielsen, J. Prospects for Microbial Biodiesel Production. *Biotechnol. J.* **2011**, *6*, 277−285.

(6) Challis, G. L.; Hopwood, D. Synergy and Contingency as Driving Forces for the Evolution of Multiple Secondary Metabolite Production by Streptomyces Species. *Proc. Natl. Acad. Sci. U.S.A.* **2003**, *100* (Suppl), 14555−14561.

(7) Le Maréchal, P.; Decottignies, P.; Marchand, C. H.; Degrouard, J.; Jaillard, D.; Dulermo, T.; Froissard, M.; Smirnov, A.; Chapuis, V.; Virolle, M. J. Comparative Proteomic Analysis of Streptomyces Lividans Wild-Type and *ppk* Mutant Strains Reveals the Importance of Storage Lipids for Antibiotic Biosynthesis. *Appl. Environ. Microbiol.* **2013**, *79*, 5907−5917.

(8) Xu, D.; Seghezzi, N.; Esnault, C.; Virolle, M. J. Repression of Antibiotic Production and Sporulation in *Streptomyces coelicolor* by Overexpression of a TetR Family Transcriptional Regulator. *Appl. Environ. Microbiol.* **2010**, *76*, 7741−7753.

(9) Naumann, D. Infrared Spectroscopy in Microbiology. *Encycl. Anal. Chem.* **2000**, 102−131.

(10) Lu, F.; Belkin, M. Infrared Absorption Nano-Spectroscopy Using Sample Photoexpansion Induced by Tunable Quantum Cascade Lasers. *Opt. Express* **2011**, *19*, 19942−19947.

(11) Felts, J. R.; Cho, H.; Yu, M.-F.; Bergman, L. a; Vakakis, A. F.; King, W. P. Atomic Force Microscope Infrared Spectroscopy on 15 nm Scale Polymer Nanostructures. *Rev. Sci. Instrum.* **2013**, *84*, 023709.

(12) Marcott, C.; Lo, M.; Kjoller, K. Differentiation of Sub-Micrometer Domains in a Poly(hydroxyalkanoate) Copolymer Using Instrumentation That Combines Atomic Force Microscopy (AFM) and Infrared (IR) Spectroscopy. *Appl. Spectrosc.* **2011**, *65*, 1145−1150.

(13) Katzenmeyer, A. M.; Aksyuk, V.; Centrone, A. Nanoscale Infrared Spectroscopy: Improving the Spectral Range of the Photothermal Induced Resonance Technique. *Anal. Chem.* **2013**, *85*, 1972−1979.
(14) Mayet, C.; Dazzi, A.; Prazeres, R.; Ortega, J. M.; Jaillard, D. In Situ Identification and Imaging of Bacterial Polymer Nanogranules by Infrared Nanospectroscopy. *Analyst* **2010**, *135*, 2540−2545.
(15) Mayet, C.; Dazzi, A.; Prazeres, R.; Allot, F.; Glotin, F.; Ortega, J. M. Sub-100 nm IR Spectromicroscopy of Living Cells. *Opt. Lett.* **2008**, *33*, 1611−1613.
(16) Dazzi, A.; Glotin, F.; Carminati, R. Theory of Infrared Nanospectroscopy by Photothermal Induced Resonance. *J. Appl. Phys.* **2010**, *107*, 1−7.
(17) Dazzi, A.; Prater, C. B.; Hu, Q.; Chase, D. B.; Rabolt, J.; Marcott, C. AFM-IR: Combining Atomic Force Microscopy and Infrared Spectroscopy for Nanoscale Chemical Characterization. *Appl. Spectrosc.* **2012**, *66*, 1365−1384.
(18) Mayet, C.; Deniset-Besseau, A.; Prazeres, R.; Ortega, J. M.; Dazzi, A. Analysis of Bacterial Polyhydroxybutyrate Production by Multimodal Nanoimaging. *Biotechnol. Adv.* **2013**, *31*, 369−374.
(19) Lahiri, B.; Holland, G.; Centrone, A. Chemical Imaging Beyond the Diffraction Limit: Experimental Validation of the PTIR Technique. *Small* **2013**, *9*, 439−445.
(20) Thomson, N.; Sivaniah, E. Synthesis, Properties and Uses of Bacterial Storage Lipid Granules as Naturally Occurring Nanoparticles. *Soft Matter* **2010**, 4045−4057.
(21) Wältermann, M.; Hinz, A.; Robenek, H.; Troyer, D.; Reichelt, R.; Malkus, U.; Galla, H.-J.; Kalscheuer, R.; Stöveken, T.; von Landenberg, P.; Steinbüchel, A. Mechanism of Lipid-Body Formation in Prokaryotes: How Bacteria Fatten Up. *Mol. Microbiol.* **2005**, *55*, 750−763.